

Equatorial Rayleigh-Taylor Instability Growth Rate Estimated Using WAM-IPE

Chun Yen Huang¹, Tzu-Wei Fang², Arthur D. Richmond³, Timothy J. Fuller-Rowell¹

¹ Cooperative Institute for Research in Environmental Sciences, University of Colorado Boulder, CO, USA

² Space Weather Prediction Center, National Oceanic and Atmospheric Administration, CO, USA

³ High Altitude Observatory, National Center for Atmospheric Research, CO, USA

Abstract: The simplify expression for Rayleigh-Taylor (R-T) growth rate is derived for direct estimation using the coupled Whole Atmosphere Model and Ionosphere Plasmasphere Electrodynamic model (WAM-IPE). The result show that the strong R-T growth rate is generated in the uplifting ionosphere structure at the magnetic equator during the post-sunset period. To further investigate the distributions and the variations of the R-T growth rate, the diurnal variation, seasonal variation, and solar activity effect are carried out. The R-T growth rates mainly appear between 1900 LT and 2200 LT, and the magnitude at 284°E is greater than that at 120°E as well as 0°E. During the high solar activity period, the R-T growth rates are more prominent in equinox seasons, and however, the greatest growth rate is found at east Pacific sector in December solstice during low solar activity period.

Rayleigh-Taylor Instability Growth Rate

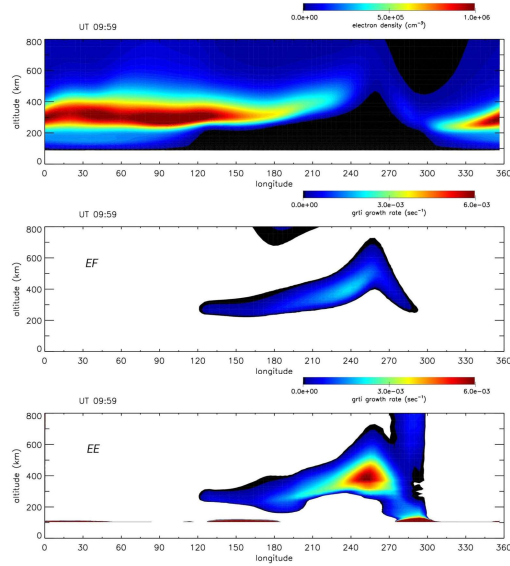


Figure 1. SAMI3 ion density (top) and R-T growth rate (bottom) as a function of geographic longitude and altitude at the magnetic equator on 10 March 2020 (F10.7 ≈ 70). EF and EE represent that the lower limit of the integral is 150 and 100 km, respectively. [Huba, 2022]

• Huba (2022) derived the generalized Rayleigh-Taylor instability (GRTI) which includes ion inertia, acceleration forces, as well as E region drivers, and use SAMI3 with thermosphere parameters specified by TIEGCM to estimate the growth rate.

• Huba (2022) concluded that inertia and acceleration forces do not significantly impact the GRTI for nominal ionospheric conditions, and inclusion of E region drivers increased the growth rate. Besides, in his result gravity is the primary driver for the instability for the EF case.

Expression for Rayleigh-Taylor Instability in Apex Coordinate

$$\frac{\partial n}{\partial t} + \nabla \cdot \left(\frac{n}{B^2} \vec{E} \times \vec{B} \right) + \nabla \cdot (n \vec{v}_i) = q - I$$

$$\Rightarrow \frac{Dn'}{Dt} - \frac{(K_x^{DF} - \Sigma_c E_y)}{\Sigma_x B_{e3} \cos^2 \lambda_m \eta} \frac{\partial \eta}{\partial y} \eta' = 0$$

$$\frac{1}{\eta_0} \frac{\partial \eta_0}{\partial y} - \frac{1}{K_x^{DF}} \frac{\partial K_x^{DF}}{\partial y} \Rightarrow \gamma = \frac{(K_x^{DF} - \Sigma_c E_y)}{K_x^{DF} \Sigma_x B_{e3} \cos^2 \lambda_m} \frac{\partial K_x^{DF}}{\partial y}$$

γ : growth rate
 Σ_c : integrated downward Pedersen conductivity
 Σ_x : integrated eastward Pedersen conductivity
 E_y : vertical electric field
 u : neutral wind
 σ_p : Pedersen conductivity
 σ_H : Hall conductivity
 η : ion flux

$$K_x^{DF} = B_{e3} \cos \lambda_m \int_{S(150)}^{N(150)} \left[\frac{\sigma_p d_1^2}{D} u_{e2} + \left(\sigma_H - \frac{\sigma_p d_1 d_2}{D} \right) u_{e1} + \frac{nm_i e_2 \cdot g}{B_{e3} B} \right] ds$$

$$K_x^{DF} = \cos \lambda_m \int_{S(150)}^{N(150)} \frac{n_0 m_i e_2 \cdot g}{B} ds$$

- The simplify function for calculating the R-T growth rate is similar with the function derived by Sultan (1996), but it has been projected to the apex coordinate. We assume that the ionosphere is stable, and the recombination effects are small above 300 km [Bittencourt and Abdu 1981]. Thus, we didn't take the recombination rate into account.
- The coupled Whole Atmosphere Model and Ionosphere Plasmasphere Electrodynamic model (WAM-IPE) applied the apex coordinate system to calculate the field-line integrated parameters, allowing for direct estimation of the R-T growth rate. The lower boundary of the integrals is 150 km.

Rayleigh-Taylor Instability Growth Rate Estimated Using WAM-IPE

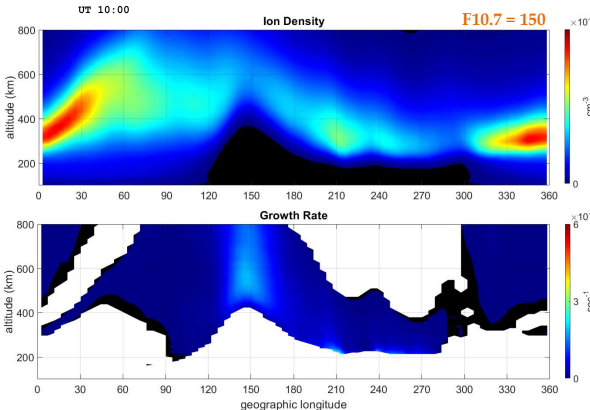


Figure 2. WAM-IPE ion density (top) and R-T growth rate at the magnetic equator at March equinox. The model is driven by F10.7=150 and Kp=1.

- The growth rate appears at the uplifting ionospheric structure which is associated the post-sunset pre-reversal enhancement vertical drift.

Acknowledgment: The authors gratefully acknowledge support from the National Science Foundation's Space Weather with Quantification of Uncertainties program under grant number AGS 2028032

Daily Variation

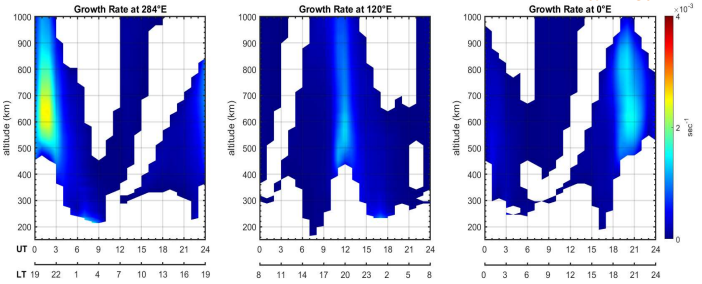


Figure 3. Daily variation of growth rate at different geographic longitude in March. From left to right panel is at 284°E, 120°E, and 0°E, respectively.

- The large growth rate can be observed at around 1900 LT ~ 2200 LT, which is consistent with previous studies [e.g., Fejer et al., 1999; Rajesh et al., 2017].

Seasonal Variation and Solar Activity Effect

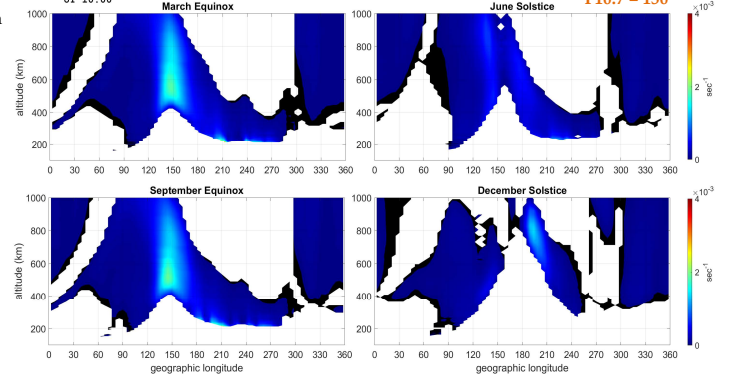


Figure 3. High solar activity of growth rate on two equinoxes and solstices at 1000 UT.

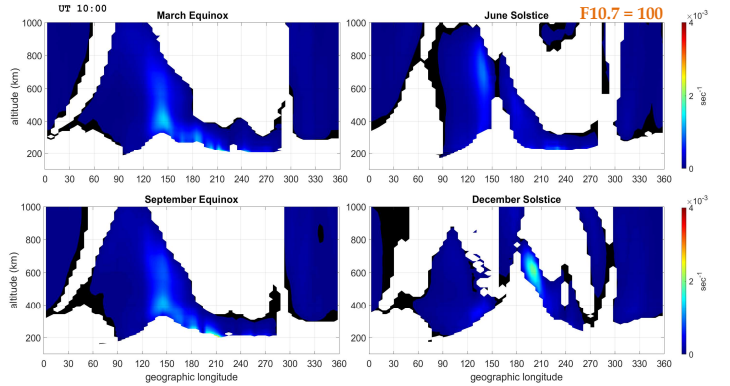


Figure 4. Same as Figure 3, but for the low solar activity.

- The growth rate in December solstice is more pronounced and latter than that in other seasons at east Pacific sector during low solar activity. We can not see the same feature in other UT plots (don't show here).

Summary

- The larger growth rates mainly appear at the post-sunset period, and the magnitudes are comparable with Huba (2022), which depicts our formula for calculating R-T instability growth rate is appropriate.
- The altitude and the magnitude of growth rate at 284°E is greater than the other two longitude region.
- The growth rates are much larger in the equinox seasons during high solar activity, and however, the greater growth rates can be observed in the December solstice during low solar activity.
- In general, the magnitudes of growth rate increasing with the increasing solar activity, except east Pacific region in December solstice.

Future Work

- With the capability to forecast ionospheric structures up to two days in advance, WAM-IPE provides us an opportunity to anticipate the Rayleigh-Taylor growth rate.
- By comparing WAM-IPE R-T growth rate with ground-based GNSS data, our ultimate goal is to explore the feasibility of future forecasting and improve prediction accuracy.